ELSEVIER

22 October 2001

Physics Letters A 289 (2001) 167–171

PHYSICS LETTERS A

www.elsevier.com/locate/pla

A robust verification of the quantum nature of light

Matteo G.A. Paris

Quantum Optics and Information Group, Istituto Nazionale per la Fisica della Materia, Universitá di Pavia, via Bassi 6, I-27100 Pavia, Italy

Received 4 May 2001; accepted 18 September 2001
Communicated by P.R. Holland

Abstract

We present a conditional experiment involving a parametric amplifier and an avalanche photodetector to generate highly nonclassical states of the radiation field. The nonclassicality is robust against amplifier gain, detector efficiency and dark counts. At the output all the generalized Wigner functions have negative values, and this is exploited in order to reveal the nonclassicality through quantum homodyne tomography.

1. Introduction

Nonclassical states of light are relevant in many fields, which ranges from fundamental tests of quantum mechanics to applications in quantum communication and measurements [1]. In the last two decades several schemes to generate different kinds of nonclassical light have been suggested, and some of them have been implemented [2]. However, with the exception of squeezing, the generation and the detection of nonclassical light is experimentally challenging [3]. The aim of this Letter is to suggest a simple scheme to verify the quantum nature of light in a state as nonclassical as a Fock number state. Remarkably, a closely related experimental realization has been recently presented [4]. The main feature of our scheme is its robustness against the possible imperfections of the setup, such as finite amplifier gain, nonunit detector efficiency and the occurrence of dark counts.

2. The vacuum free state

Let us consider an active $\chi^{(2)}$ crystal operating as a nondegenerate parametric amplifier (NOPA, for details of the experimental setup see the end of the Letter). The NOPA, pumped at frequency $\omega_P = \omega_a + \omega_b$, couples two modes a and b (idler and signal modes) via the medium nonlinearity. In the rotating-wave approximation, the evolution operator of the NOPA under phase-matching conditions can be written as $U_\lambda = \exp[\lambda(a^\dagger b^\dagger - ab)]$, where the "gain" λ is proportional to the interaction time, the nonlinear susceptibility, and the pump intensity. For vacuum input, we have spontaneous parametric down-conversion and the output state is given by the twin-beam

$$|\psi\rangle = \sqrt{1-\xi^2}\sum_{n=0}^{\infty}\xi^n|n\rangle_a \otimes |n\rangle_b, \quad \xi = \tanh\lambda. \tag{1}$$

We now consider the situation in which one of the two beams (say, mode b) is revealed by an ideal avalanche on/off photodetector, i.e., a detector which has no output when no photon is detected and a fixed output

E-mail address: paris@unipv.it (M.G.A. Paris).

0375-9601/01/$ – see front matter
PII: S0375-9601(01)00618-1

when one or more photons are detected. The action of an on/off detector is described by the two-value POVM,

$$\hat{\Pi}_0 \doteq \sum_{k=0}^{\infty} (1-\eta_A)^k |k\rangle\langle k|, \qquad \hat{\Pi}_1 \doteq \hat{\mathbf{I}} - \hat{\Pi}_0, \tag{2}$$

η_A being the quantum efficiency. The outcome "1" (i.e., registering a "click" corresponding to one or more incoming photons) occurs with probability

$$P_1 = \langle\psi|\hat{\mathbf{I}} \otimes \hat{\Pi}_1|\psi\rangle = \frac{\eta_A \xi^2}{1-\xi^2(1-\eta_A)} \tag{3}$$

and, correspondingly, the conditional output state for the mode a is given by

$$\hat{\varrho}_1 = \frac{1}{P_1} \mathrm{Tr}_b\big[|\psi\rangle\langle\psi| \hat{\mathbf{I}} \otimes \hat{\Pi}_1\big]. \tag{4}$$

In the Fock basis we have

$$\hat{\varrho}_1 = \frac{1-\xi^2}{P_1} \sum_{k=1}^{\infty} \xi^{2k}\big[1-(1-\eta)^k\big]|k\rangle\langle k|. \tag{5}$$

The density matrix in Eq. (5) describes a *pseudo*-thermal state, where the vacuum component has been removed by the conditional measurement. Such a state is highly nonclassical, as also discussed in Ref. [5]. In the limit of low gain $\lambda \ll 1$ the conditional state $\hat{\varrho}_1$ approaches the number state $|1\rangle\langle 1|$ with one photon. The Wigner function $W(\alpha)$ of state (4) exhibits negative values for any gain λ and quantum efficiency η_A. In particular, in the origin of the phase space we have

$$W(0) = -\frac{2}{\pi} \frac{1-\xi^2}{1+\xi^2} \frac{1-\xi^2(1-\eta_A)}{1+\xi^2(1-\eta_A)}. \tag{6}$$

One can see that also the generalized Wigner function for s-ordering $W_s(\alpha) = -2/(\pi s) \int d^2\gamma\, W_0(\gamma) \times \exp[2/s|\alpha-\gamma|^2]$ shows negative values for $s \in (-1, 0)$. In particular, one has

$$W_s(0) = -\frac{2(1+s)}{\pi} \frac{(1-\xi^2)}{(1-s)+\xi^2(1+s)} \times \frac{1-\xi^2(1-\eta_A)}{(1-s)+\xi^2(1+s)(1-\eta_A)}. \tag{7}$$

If we take as a measure of nonclassicality the lowest index s^* for which W_s is a well-behaved probability (regular, positive-definite) [6], Eq. (7) says that for $\hat{\varrho}_1$ we have $s^* = -1$, i.e., $\hat{\varrho}_1$ describes a state as nonclassical as a number state.

The fact that all the generalized Wigner functions have negative values may be exploited in order to reveal the nonclassicality of $\hat{\varrho}_1$ through quantum homodyne tomography. In fact, one has

$$W_s(0) = \mathrm{Tr}\big[\hat{\varrho}_1 \hat{W}_s\big],$$

$$\hat{W}_s = \frac{2}{\pi} \frac{1}{1-s} \left(\frac{s+1}{s-1}\right)^{a^\dagger a}, \tag{8}$$

and, therefore [7],

$$W_s(0) = \int dx\, p_{\eta_H}(x) R_{\eta_H}\big[\hat{W}_s\big](x), \tag{9}$$

where $p_{\eta_H}(x)$ is the probability distribution of a random phase homodyne detection (with quantum efficiency η_H) and $R_{\eta_H}[\hat{W}_s](x)$ is the tomographic kernel for the operator $\hat{W}_s$, which is given by [8]

$$R_{\eta_H}\big[\hat{W}_s\big](x) = \frac{2\eta_H}{\pi} \frac{\Phi\big(1; 1/2; -\frac{2\eta_H x^2}{(1-s)\eta_H - 1}\big)}{(1-s)\eta_H - 1}, \tag{10}$$

where $\Phi(a, b; z)$ is the confluent hypergeometric function. $R_{\eta_H}[\hat{W}_s](x)$ is a bounded function for $s < 1 - \eta_H^{-1}$ which represents the maximum index of the Wigner function $W_s(0)$ that can be reconstructed by homodyne tomography with efficiency η_H. In Fig. 1 we show a typical reconstruction of $W_s(0)$ for different values of s, λ and η_A.

3. Inclusion of dark counts

Besides quantum efficiency, i.e., lost photons, the performance of a realistic photodetector are also degraded by the presence of dark-count, i.e., by "clicks" that do not correspond to any incoming photon. In order to take into account both these effects we use the simple scheme depicted in Fig. 2.

A real photodetector is modeled as an ideal photodetector (unit quantum efficiency, no dark-count) preceded by a beam splitter (of transmissivity equal to the quantum efficiency η) whose second port is in an auxiliary excited state $\hat{\nu}$, which can be a thermal state, or a phase-averaged coherent state, depending on the kind of background noise (a thermal or Poissonian). If the second port of the beam splitter is the vacuum $\hat{\nu} = |0\rangle\langle 0|$ we have no dark-count and the POVM of the photodetector reduces to that of Eq. (2). For the second port of the BS excited in a generic mixture

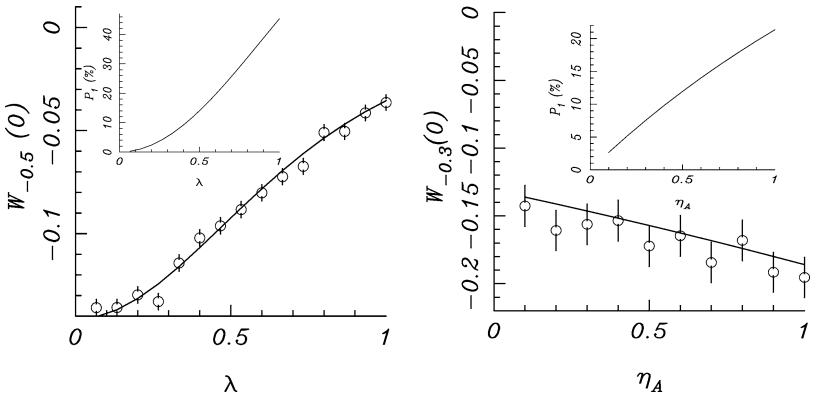

Fig. 1. Reconstruction of the Wigner function in the origin of the phase-space by (Monte Carlo simulated) homodyne tomography (sample of 5×10^4 data at random phase). Left: reconstruction of $W_{-0.5}(0)$ versus gain λ, for $\eta_A = 60\%$ and $\eta_H = 70\%$. Right: reconstruction of $W_{-0.3}(0)$ versus the avalanche photodetector quantum efficiency η_A, for $\lambda = 0.5$ and homodyne quantum efficiency $\eta_H = 80\%$. In both plots the solid line is the theoretical value, and the inset shows the detection probability P_1.

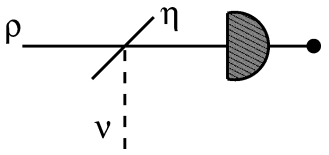

Fig. 2. Model for a realistic photodetector.

$\hat{\nu} = \sum_s \nu_{ss} |s\rangle\langle s|$ the POVM for the on/off photodetection is given by ($\hat{\Pi}_1 \doteq \hat{\mathbf{I}} - \hat{\Pi}_0$)

$$\hat{\Pi}_0 = \sum_{n=0}^{\infty} (1-\eta)^n \sum_{s=0}^{\infty} \nu_{ss} \eta^s \binom{n+s}{s} |n\rangle\langle n|. \tag{11}$$

The density matrices of a thermal state and a phase-averaged coherent state (with M mean photons) are given by

$$\hat{\nu}_T = \frac{1}{M+1} \sum_s \left(\frac{M}{M+1} \right)^s |s\rangle\langle s|, \tag{12}$$

$$\hat{\nu}_P = e^{-M} \sum_s \frac{M^s}{s!} |s\rangle\langle s|. \tag{13}$$

In order to reproduce a background noise with mean photon number N we consider the state $\hat{\nu}$ with average photon number $M = N/(1-\eta_A)$. In these case we have

$$\hat{\Pi}_0^T = \frac{1}{1+N} \sum_n \left(1 - \frac{\eta_A}{1+N} \right)^n |n\rangle\langle n|, \tag{14}$$

$$\hat{\Pi}_0^P = e^{-N} \sum_n \left[(1-\eta_A)^n L_n\left(-N \frac{\eta_A}{1-\eta_A} \right) \right] |n\rangle\langle n|, \tag{15}$$

where T and P denotes thermal and Poissonian, respectively, and $L_n(x)$ is the Laguerre polynomial of order n. The corresponding detection probabilities are given by

$$P_1^T = 1 - \frac{1-\xi^2}{[1+N](1-\xi^2) + \eta_A \xi^2}, \tag{16}$$

$$P_1^P = 1 - \frac{1-\xi^2}{1-\xi^2(1-\eta_A)} \times \exp\left[-N \frac{1-\xi^2}{1-\xi^2(1-\eta_A)} \right]. \tag{17}$$

For small N the two models lead to the same detection probability at the first order in N, $P_1^T \simeq P_1^P = P_1 + O[N^2]$, with

$$P_1 = \frac{\eta_A \xi^2}{1-\xi^2(1-\eta_A)} + \frac{(1-\xi^2)^2}{[1-\xi^2(1-\eta_A)]^2} N. \tag{18}$$

In the following we will use the Poissonian background, and omit the index P. The conditional output state, after the observation of a click, is now given by

$$\hat{\varrho}_1 = \frac{1}{P_1} (1-\xi^2)$$

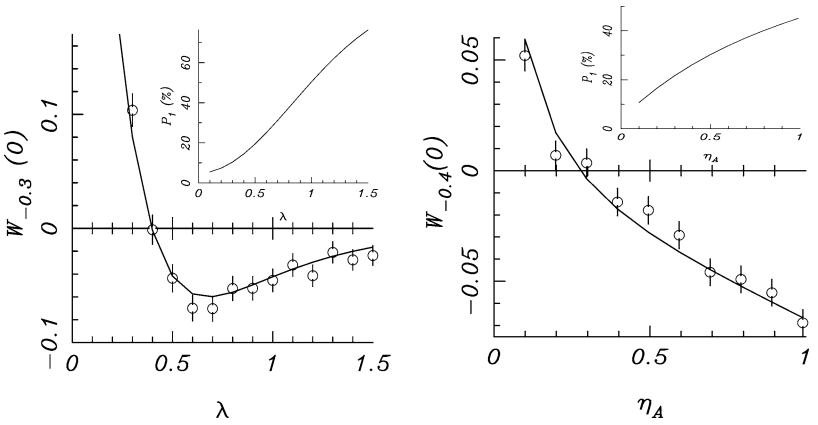

Fig. 3. Reconstruction of the Wigner function in the origin of the phase-space by (Monte Carlo simulated) homodyne tomography (sample of 5×10^4 data at random phase). Left: reconstruction of $W_{-0.3}(0)$ versus gain λ, for $\eta_A = 70\%$, $\eta_H = 80\%$, and $N = 0.05$. Right: reconstruction of $W_{-0.4}(0)$ versus quantum efficiency η_A for $\lambda = 0.8$, $\eta_H = 75\%$, and $N = 0.08$. In both plots the solid line is the theoretical value, and the inset shows the detection probability P_1. Increasing N would generally need a larger threshold for η_A.

$$\times \sum_n \xi^{2n} \left[1 - \frac{(1-\eta_A)^n}{e^N} L_n\left(-\frac{N\eta_A}{1-\eta_A} \right) \right] \times |n\rangle\langle n| \tag{19}$$

and the generalized Wigner function $W_s(0)$ in the origin of the phase space is

$$W_s(0) = \frac{2(1-\xi^2)}{\pi P_1} \left\{ \frac{1}{(1-s)+\xi^2(1+s)} - \frac{\exp\left[-N \frac{(1+s)+2\xi^2(1+s)(1-\eta_A)}{(1+s)+\xi^2(1+s)(1-\eta_A)} \right]}{(1-s)+\xi^2(1-\eta_A)(1+s)} \right\}. \tag{20}$$

The Wigner function $W(0)$ for $s = 0$ (as well as for $s < 0$) is no longer negative for all values of parameters. On the other hand, there is a large range of values of the quantum efficiency η_A and the gain λ giving negative $W_s(0)$ with s accessible by homodyne tomography with realistic values of the homodyne efficiency η_H. In other words, the generation and the detection of nonclassicality are robust also against the occurrence of dark counts in the avalanche conditioning photodetector. In Fig. 3 we show a typical reconstruction of $W_s(0)$ for different values of parameters.

4. About the experimental implementation

In a practical implementation the NOPA consists of a type-II phase-matched KTP crystal that is pumped by the second harmonic of a Q-switched and mode-locked Nd:YAG laser. Previously, such a NOPA has been employed with parametric gains > 10 ($|\xi|^2 > 0.9$), to generate highly quantum-correlated twin-beams of light at 1064 nm [9]. By appropriately choosing the input quantum state, a similar setup was then used to demonstrate the production of squeezed-vacuum state with a high degree (5.8 ± 0.2 dB) of squeezing [10]. In the present context, the twin-beams, which are easily separable because of their orthogonal polarizations resulting from type-II phase matching, can be separately detected; beam a with a homodyne detector to verify nonclassicality, and beam b with an avalanche photodetector. The main challenge in the present experiment is the achievement of high degrees of overlap (mode-matching efficiency) between the down-converted and the LO modes. Such overlap is nontrivial in pulsed, traveling-wave experiments owing to the distortion of the down-converted modes that is caused by the spatio-temporally Gaussian profile of the pump beam. The mode mismatch results in a decreased overall quantum efficiency. However, with suitable choice of LOs, $\eta_H > 70\%$ has been achieved [11], an adequate value for the present experiment (cf. Figs. 1 and 3). In the measurements on beam b, the main challenge will be the selection of the appropriate mode, which can be performed by exploiting quantum-frequency conversion, a process that has been previously demonstrated [12].

5. Conclusions

In conclusion, we presented a robust experiment to verify the quantum nature of light. This goal is achieved by a conditional scheme, where one of the entangled twin-beam exiting a NOPA is revealed by an avalanche photodetector, leaving the other one in a pseudo-thermal state with no vacuum component. The nonclassicality, as well as its verification by homodyne tomography, are robust against amplifier gain, detector efficiency and dark counts.

Acknowledgements

This work has been cosponsored by MURST (Project "Amplificazione e rivelazione di radiazione quantistica") and INFM (PAIS-TWIN). The author would thank Mauro D'Ariano for many useful discussions, and Prem Kumar for remarks on the experimental implementation.

References

[1] See, for example, F. De Martini, G. Denardo, L. Hardy (Eds.), Quantum Interferometry III, Fort. Phys. 48 (2000), special issue;
P. Kumar, G.M. D'Ariano, O. Hirota (Eds.), Quantum Communication, Computing and Measurement II, Kluwer Academic, 2000.
[2] See, for example, the special issues: Quantum State Preparation and Measurement, J. Mod. Opt. 44 (1997);
Quantum Optics and Quantum Information, Acta Phys. Slov. 48 (1998).
[3] T. Opatrny, D.-G. Welsch, Prog. Opt. XXXIX (1999) 63.
[4] A.I. Lvovsky et al., Phys. Rev. Lett. 87 (2001) 050402.
[5] L. Mandel, E. Wolf, Optical Coherence and Quantum Optics, Cambridge University Press, 1995, p. 625.
[6] C.T. Lee, Phys. Rev. 44 (1991) R2275.
[7] G.M. D'Ariano, in: T. Hakioğlu, A.S. Shumovsky (Eds.), Quantum Optics and the Spectroscopy of Solids, Kluwer Academic, 1997, p. 175.
[8] G.M. D'Ariano, in: O. Hirota, A.S. Holevo, C.M. Caves (Eds.), Quantum Communication, Computing and Measurement, Plenum, New York, 1997, pp. 253–264.
[9] O. Aytür, P. Kumar, Phys. Rev. Lett. 65 (1990) 1551.
[10] C. Kim, P. Kumar, Phys. Rev. Lett. 73 (1994) 1605.
[11] O. Aytür, P. Kumar, Opt. Lett. 17 (1992) 529.
[12] J. Huang, P. Kumar, Phys. Rev. Lett. 68 (1992) 2153.